

# $p$ – $\rho$ – $T$ Behavior of Four Lean Synthetic Natural-Gas-Like Mixtures from 250 K to 450 K with Pressures to 37 MPa

Mark O. McLinden\*

Thermophysical Properties Division, National Institute of Standards and Technology, 325 Broadway, Mailstop 838.07, Boulder, Colorado 80305, United States

**S** Supporting Information

**ABSTRACT:** The  $p$ – $\rho$ – $T$  behaviors of four lean synthetic natural gas mixtures were measured along isotherms of 250 K, 350 K, and 450 K with pressures to 37 MPa with a two-sinker, magnetic-suspension densimeter. The gravimetrically prepared mixtures have seven to nine components (methane to pentane). They are all nominally 0.90 mole fraction methane, and they differ primarily in the amount of pentane and isopentane and the presence or absence of nitrogen and carbon dioxide. The analysis for density accounts for the force transmission error in the magnetic suspension coupling (MSC) of the densimeter and the magnetic effects of the fluid. These data are compared to the GERG 2004 and AGA-8 models for natural gas mixtures. The densities calculated by both the models are generally in very good agreement with the data, with average deviations less than 0.05 %, at the higher temperatures ( $T = 350$  K and  $T = 450$  K) and lower pressures ( $p < 15$  MPa). But at higher pressures and lower temperatures, the average deviations are substantially larger, ranging up to 0.28 % and 0.93 % for the GERG 2004 and AGA-8 models, respectively, for  $T = 250$  K and  $p > 15$  MPa for one or more of the mixtures. Additional data on these same mixtures were measured by Texas A&M University and are reported in a previous paper.

## 1. INTRODUCTION

The National Institute of Standards and Technology (NIST) is cooperating with Texas A&M University in a project to measure the properties of natural gas systems and evaluate the adequacy of the models commonly used in the gas industry. The properties of greatest industrial interest are the phase boundaries and the  $p$ – $\rho$ – $T$  (density) and speed of sound behavior. Knowledge of the phase boundaries is important to avoid condensation in pipelines. The density and sound speed data relate to flow metering, allowing the measurand from a flow meter (e.g., a volumetric flow rate) to be converted to a mass flow rate. Many natural gases are complex, multicomponent mixtures, yet accurate experimental data on multicomponent mixtures are relatively scarce, and the models are based largely on binary mixture data.

The present paper describes high-accuracy measurements of the  $p$ – $\rho$ – $T$  behavior of four lean (i.e., a gas with no heavy components), multicomponent, synthetic natural-gas-like mixtures with pressures to 37 MPa. The measurements were made with a two-sinker densimeter. Comparisons of the data to the two most comprehensive and widely used models for natural gas systems, namely, the GERG-2004<sup>1</sup> model sponsored by the Groupe European de Recherches Gazieres and the AGA-8 model<sup>2</sup> sponsored by the American Gas Association, are presented. Texas A&M has measured the phase boundaries and the  $p$ – $\rho$ – $T$  behavior at pressures up to 180 MPa; these data are reported by Atilhan et al.<sup>3</sup>

## 2. EXPERIMENTAL SECTION

**2.1. Experimental Samples.** The four synthetic, natural-gas-like mixtures studied in this work were prepared gravimetrically by a commercial laboratory, Accurate Gas Products, LLC of

Lafayette, LA (Please note: certain trade names and vendors are identified only to adequately document the experimental procedures. This does not constitute a recommendation or endorsement by the National Institute of Standards and Technology, nor does it imply that they are necessarily the best available for the purpose). The compositions are listed in Table 1, and they are designated as SNG-1 through SNG-4. The mixtures are all nominally 0.90 mole fraction methane, and they differ primarily in the amount of pentane and isopentane and the presence or absence of nitrogen and carbon dioxide. The vendor did not provide an uncertainty statement for the composition, but we estimate the standard ( $k=1$ ) uncertainty to be 0.00005 mass fraction for each component, based on the resolution of the balance used by the vendor and their method of sequentially loading and weighing each component into the sample cylinder. The same sample cylinders discussed in the paper by Texas A&M University were measured here.

**2.2. Apparatus Description.** The present measurements utilized a two-sinker densimeter with a magnetic suspension coupling (MSC). This type of instrument applies the Archimedes (buoyancy) principle to provide an absolute determination of the density. This general type of instrument is described by Wagner and Kleinrahm,<sup>4</sup> and our instrument is described in detail by McLinden and Lösch-Will.<sup>5</sup> Briefly, two sinkers of nearly the same mass and surface area, but very different volumes, are each weighed with a high-precision balance while they are immersed in a fluid of unknown density. The fluid density  $\rho$  is

**Received:** December 21, 2010

**Accepted:** January 24, 2011

**Published:** February 18, 2011



**Table 1. Reported Compositions (Molar Fraction) and Average Molar Mass of the Studied Mixtures**

component	mixture			
	SNG-1	SNG-2	SNG-3	SNG-4
methane	0.89990	0.89982	0.89975	0.90001
ethane	0.03150	0.03009	0.02855	0.04565
propane	0.01583	0.01506	0.01427	0.02243
isobutane	0.00781	0.00752	0.00709	0.01140
<i>n</i> -butane	0.00790	0.00753	0.00722	0.01151
isopentane	0.00150	0.00300	0.00450	0.00450
<i>n</i> -pentane	0.00150	0.00300	0.00450	0.00450
nitrogen	0.01699	0.01697	0.01713	
carbon dioxide	0.01707	0.01701	0.01699	
M/g·mol <sup>-1</sup>	18.439	18.536	18.631	18.781

given by

$$\rho = \frac{(m_1 - m_2) - (W_1 - W_2)}{(V_1 - V_2)} \quad (1)$$

where  $m$  and  $V$  are the sinker mass and volume,  $W$  is the balance reading, and the subscripts refer to the two sinkers. Each sinker had a mass of 60 g; one was made of tantalum and the other of titanium. The MSC transmitted the gravity and buoyancy forces on the sinkers to the balance, thus isolating the fluid sample (which may be at high pressure and high temperature) from the balance. In comparison with other buoyancy techniques, the main advantage of the two-sinker method is that systematic errors in the weighing and from other sources approximately cancel.

In addition to the sinkers, two calibration masses (designated  $m_{\text{cal}}$  and  $m_{\text{tare}}$ ) are also weighed. This provides a calibration of the balance and also the information needed to correct for magnetic effects as described by McLinden et al.<sup>6</sup> The weighings yield a set of four equations that are solved to yield a balance calibration factor  $\alpha$  and a parameter  $\beta$  related to the balance tare (i.e., the magnets and other elements of the system that are always weighed). This analysis yields the fluid density in terms of directly measured quantities:

$$\rho_{\text{fluid}} = \left[ (m_1 - m_2) - \frac{(W_1 - W_2)m_1}{W_1 - \alpha\beta} \right] / \left[ (V_1 - V_2) - \frac{(W_1 - W_2)V_1}{W_1 - \alpha\beta} \right] - \rho_0 \quad (2)$$

where the  $\rho_0$  is the indicated density when the sinkers are weighed in vacuum. In other words  $\rho_0$  is an “apparatus zero.” The key point of the analysis by McLinden et al.<sup>6</sup> is that the density given by eq 2 compensates for the magnetic effects of both the apparatus and the fluid being measured.

The temperature was measured with a 25  $\Omega$  standard platinum resistance thermometer (SPRT) and resistance bridge referenced to a thermostatted standard resistor. Pressures were measured with one of three vibrating-quartz-crystal type pressure transducers having full-scale pressure ranges of 2.8 MPa, 13.8 MPa, or 68.9 MPa. Most of the measurements used the “high-range” transducer. A limited number of measurements at lower densities used the “low-range” or “medium-range” transducer. The transducers

and pressure manifold were thermostatted to minimize the effects of variations in laboratory temperature.

**2.3. Measured  $p$ – $\rho$ – $T$  Data.** Measurements were carried out along isotherms. The initial pressure was (35 to 37) MPa for most of the isotherms. Isotherms at 250 K, 350 K, and 450 K were measured for each mixture. An additional isotherm at 275 K was measured for the mixture SNG-3. For the measurements at 250 K on SNG-3, the sample was loaded to a pressure of approximately 30 MPa with the measuring cell at  $T = 300$  K; the temperature was then reduced to slightly below the target temperature, and the rest of the sample was loaded to the desired starting pressure. This was done to avoid crossing the two-phase region during loading. Three or more replicate density determinations, each requiring approximately 12 min, were made at each pressure before venting a portion of the sample to step to a lower pressure. The system was allowed to re-equilibrate approximately 120 min between pressures before resuming measurements. The temperature and pressure were measured nine times for a single density determination, and average values of  $T$  and  $p$  are reported. Eight or more pressure steps were measured along each isotherm with a final pressure of approximately 4 MPa, except that several isotherms were extended to pressures as low as 0.6 MPa. The cell was evacuated at the end of each isotherm before loading the sample for the next isotherm. Typical values of pressure along an isotherm were  $p = 35$  MPa, 30 MPa, 25 MPa, 20 MPa, 16 MPa, 12 MPa, 10 MPa, 7 MPa, and 4 MPa.

Measurements in vacuum were carried out regularly to check the zero of the pressure transducer and to determine the parameter  $\rho_0$  in eq 2. This was done between every two or three isotherms.

### 3. UNCERTAINTY ANALYSIS

McLinden and Lösch-Will<sup>5</sup> provide an analysis of uncertainties for gas-phase measurements, and McLinden and Splett<sup>7</sup> provide a further detailed uncertainty analysis for this instrument. Those results are summarized here.

The uncertainty in the density calculated with eq 2 arises from uncertainties in the sinker volumes ( $V_1$ ,  $V_2$ ), weighings of the sinkers and calibration masses ( $W_1$ ,  $W_2$ ,  $W_{\text{cal}}$ ,  $W_{\text{tare}}$ ), knowledge of the sinker masses ( $m_1$ ,  $m_2$ ) and calibration masses ( $m_{\text{cal}}$ ,  $m_{\text{tare}}$ ), and the apparatus zero ( $\rho_0$ ). Uncertainties in the volumes of the calibration masses ( $V_{\text{cal}}$ ,  $V_{\text{tare}}$ ) and the density of the nitrogen purge gas in the balance chamber have an insignificant contribution because  $V_{\text{cal}} \approx V_{\text{tare}}$ . The uncertainties in the sinker volumes  $V_1$  and  $V_2$  dominate the overall uncertainty in density. The volumes of the sinkers were calibrated at 293.15 K and atmospheric pressure by the hydrostatic comparator method described by McLinden and Splett.<sup>7</sup> The volumes at other temperatures and pressures were calculated using the linear thermal expansion coefficient of tantalum and titanium and literature values for the bulk modulus. These volumes were further adjusted by the method of Moldover and McLinden.<sup>8</sup> The combined standard ( $k = 1$ ) uncertainty in the sinker volume difference ( $V_1 - V_2$ ) is estimated to be  $16 \cdot 10^{-6} \cdot (V_1 - V_2)$  at 293 K and atmospheric pressure increasing to  $42 \cdot 10^{-6} \cdot (V_1 - V_2)$  at 450 K and 37 MPa.

At low densities, errors in the weighings have a significant effect on the uncertainty in density. The standard deviations observed in replicate weighings ranged from 0.2  $\mu\text{g}$  to 5.2  $\mu\text{g}$  for the different objects, and these contribute an uncertainty in density of 0.0005  $\text{kg} \cdot \text{m}^{-3}$ . The uncertainty in the object masses ranged from 21  $\mu\text{g}$  to 50  $\mu\text{g}$ . Because of the differential nature of

the two-sinker method, these contribute only  $2 \cdot 10^{-6}$  to the relative uncertainty in density.

The MSC transmits the buoyancy force on the sinkers to the balance; therefore, any magnetic materials near the MSC will affect the density measurement. This effect is known as a "force transmission error".<sup>6</sup> The analysis of McLinden et al.<sup>6</sup> demonstrated that such errors can be accounted for, reducing the standard uncertainty from this effect to  $2 \cdot 10^{-6} \rho$ . This effect is characterized by a "coupling factor"  $\phi$ , which expresses the efficiency of the force transmission of the MSC. For the present measurements  $\phi$  varied from 1.000022 in vacuum to 0.999993 for the gas at the highest densities.

The standard ( $k = 1$ ) uncertainty in the density is

$$\frac{u(\rho)}{\text{kg} \cdot \text{m}^{-3}} = \left[ \{16\}^2 + \{0.20|(T/\text{K} - 293)|\}^2 + \{0.63p/\text{MPa}\}^2 \right]^{0.5} \frac{10^{-6} \rho}{\text{kg} \cdot \text{m}^{-3}} + 0.0007 \quad (3)$$

where the term in brackets is from the sinker volume uncertainty, and the final, constant term includes all other uncertainties.

The SPRT used to measure the temperature of the fluid was calibrated on ITS-90 from (83 to 505) K by use of fixed point cells (argon triple point, mercury triple point, water triple point, indium freezing point, and tin freezing point). This was done as a system calibration using the same lead wires, standard resistor, and resistance bridge that were used during the measurements. The standard uncertainty of the temperature, including the uncertainty in the fixed point cells, drift in the SPRT and standard resistor, and any temperature gradients, is 2 mK.

The uncertainty of the pressure arises from three sources: the calibration of the transducers, the repeatability and drift of the transducers, and the uncertainty of the hydrostatic head correction. The pressure transducers were calibrated with piston gauges. This calibration was done in situ by connecting the piston gauge to the sample port of the filling and pressure manifold. The pressure uncertainty arising from the hydrostatic head correction is estimated to be less than  $2 \cdot 10^{-6} p$ . We estimate the standard ( $k = 1$ ) uncertainty in pressure to be  $(20 \cdot 10^{-6} \cdot p + 0.004 \text{ kPa})$  for the low-range transducer,  $(20 \cdot 10^{-6} \cdot p + 0.02 \text{ kPa})$  for the midrange transducer, and  $(26 \cdot 10^{-6} \cdot p + 0.2 \text{ kPa})$  for the high-range transducer. The complete data tables in the Supporting Information of this paper indicate which transducer was used for a given measurement.

To the above uncertainty estimates are added the standard deviations actually observed in the multiple temperature, pressure, and balance readings made over the 12 min necessary to complete a single density determination.

For purposes of comparing  $p$ - $\rho$ - $T$  data to a model, it is customary to assume that the temperature, pressure, and composition are known exactly and to lump all uncertainties into a single value for the density. The effect arising from uncertainties in the composition  $u(x_i)$  of the  $n$ -component mixture is approximated by assuming that the density can be represented by a simple virial expansion (with the further assumption that the virial coefficients are independent of small changes in composition) so that the density uncertainty due to uncertainties in the composition is simply related to the uncertainty in the molar

mass of the mixture:

$$u(\rho(x)) = \left\{ \sum_{i=1}^n \left[ \frac{\partial \rho}{\partial x_i} u(x_i) \right]^2 \right\}^{0.5} = \frac{\partial}{\partial M} \left\{ \frac{p}{RT} [1 + B\rho + C\rho^2] \right\} u(M) \quad (4)$$

The uncertainty in the molar mass of the mixture from the uncertainty in a single  $x_i$  is given by

$$u(M) = \frac{\partial M}{\partial x_i} u(x_i) = \left[ M \left( 1 - \frac{M}{M_i} \right) u(x_i) \right] \quad (5)$$

where  $M_i$  is the molar mass of an individual component, and the composition  $x_i$  and density  $\rho$  are on a mass basis. Combining eqs 4 and 5 and summing over the  $n$  components yields

$$u(\rho(x)) = \left\{ \sum_{i=1}^n \left\{ \frac{pM}{RT} [1 + B\rho + C\rho^2] \left[ 1 - \frac{M}{M_i} \right] u(x_i) \right\}^2 \right\}^{0.5} \quad (6)$$

The first terms in the summation in eq 6 are recognized as just the original approximation for the density. Considering the very approximate nature of the composition uncertainties, these approximations do not substantially impact the analysis.

The overall combined, or state-point, uncertainty is given by

$$u_C(\rho) = \left\{ \begin{aligned} & [u(\rho)]^2 + \left[ \left( \frac{\partial \rho}{\partial p} \right)_T u(p) \right]^2 + \left[ \left( \frac{\partial \rho}{\partial T} \right)_p u(T) \right]^2 \\ & + \sum_{i=1}^n \left[ \rho \left( 1 - \frac{M}{M_i} \right) u(x_i) \right]^2 \end{aligned} \right\}^{0.5} \quad (7)$$

where  $u_C$  designates the combined uncertainty, the  $u$  are the individual uncertainties, and the derivatives are evaluated from the GERG model. A composition uncertainty of 0.00005 mass fraction for each component (i.e., an uncertainty of 50 mg for the mass of each component out of a total sample mass of 1 kg) results in a nearly constant relative uncertainty in density for a given mixture, ranging from 0.0079 % to 0.0086 % ( $k = 1$ ); this is significantly larger than the experimental temperature, pressure, and density uncertainties for most conditions.

#### 4. RESULTS AND COMPARISON TO THE GERG-2004 AND AGA-8 MODELS

Tables 2 to 5 present data measured along the isotherms. The values listed in the tables represent an average of the replicate measurements at a given  $(T, p)$  state. (The comparison figures and statistics are based on all the points, however.) The final two columns give the relative difference between the measured densities and the GERG-2004 and AGA-8 models for natural gas systems:

$$\Delta_{\text{GERG}} = 100 \frac{\rho - \rho_{\text{GERG}}}{\rho_{\text{GERG}}} \quad (8)$$

and

$$\Delta_{\text{AGA}} = 100 \frac{\rho - \rho_{\text{AGA}}}{\rho_{\text{AGA}}} \quad (9)$$

**Table 2.** Experimental  $p$ – $\rho$ – $T$  Data for Mixture SNG-1 and Relative Deviations of the Experimental Data  $\rho$  from Densities Calculated with the GERG-2004  $\rho_{\text{GERG}}$  and AGA-8  $\rho_{\text{AGA}}$  Models<sup>a</sup>

$T$ K	$p$ MPa	$\rho$ kg·m <sup>-3</sup>	$\Delta_{\text{GERG}}$	$\Delta_{\text{AGA}}$
449.993	37.3445	168.608	0.0121	-0.0034
449.995	34.8870	160.003	0.0112	-0.0094
449.995	28.7350	136.596	0.0143	-0.0236
449.995	23.8489	116.062	0.0188	-0.0301
449.996	19.9245	98.382	0.0179	-0.0332
449.997	15.8406	79.027	0.0215	-0.0255
449.998	11.4483	57.397	0.0223	-0.0165
449.998	9.8041	49.161	0.0227	-0.0129
449.998	7.6333	38.229	0.0206	-0.0110
449.999	3.9336	19.590	0.0172	-0.0064
449.999	1.9224	9.528	0.0153	-0.0005
350.001	36.8612	227.799	0.0252	-0.0743
350.002	29.2728	195.314	0.0101	-0.0552
350.003	25.1680	173.794	-0.0018	-0.0575
350.002	20.1058	142.853	-0.0111	-0.0731
350.001	15.7478	112.613	-0.0133	-0.0788
350.001	11.6389	82.221	-0.0043	-0.0616
350.000	9.7019	67.738	-0.0006	-0.0514
350.000	9.5562	66.651	-0.0029	-0.0530
350.000	6.9755	47.641	-0.0016	-0.0411
350.000	3.8889	25.756	0.0023	-0.0224
350.000	2.9617	19.417	0.0026	-0.0175
350.000	1.9764	12.814	0.0020	-0.0128
350.000	1.9436	12.597	0.0009	-0.0137
349.999	1.5970	10.310	0.0013	-0.0115
349.999	1.1940	7.672	0.0013	-0.0091
349.999	0.7931	5.072	0.0014	-0.0067
349.999	0.5860	3.739	-0.0052	-0.0118
250.001	2.1419	20.772	-0.1527	-0.2377
249.999	1.5833	15.005	0.0492	-0.0148
250.001	1.1901	11.086	0.0367	-0.0126
250.000	0.7848	7.186	0.0283	-0.0057
250.001	0.5938	5.395	0.0223	-0.0042
250.002	34.9495	328.877	0.1283	-0.3500
250.000	29.6354	313.469	0.1346	-0.3986
250.000	24.2049	292.822	0.1093	-0.4689
250.000	19.7273	269.051	0.0452	-0.5504
250.000	15.9138	239.061	-0.0892	-0.6853
250.000	11.9906	187.819	-0.2937	-0.8815
249.999	10.0204	150.234	-0.2241	-0.8622
250.000	7.9700	107.685	0.0049	-0.5565

<sup>a</sup>Data are presented in the sequence in which they were measured; blank lines separate different sample fillings.

There was very little point-to-point variation between the replicates, as detailed in the Supporting Information. The quality of the fit will be expressed in terms of the average absolute deviations (AADs) between the experimental data and the

**Table 3.** Experimental  $p$ – $\rho$ – $T$  Data for Mixture SNG-2 and Relative Deviations of the Experimental Data  $\rho$  from Densities Calculated with the GERG-2004  $\rho_{\text{GERG}}$  and AGA-8  $\rho_{\text{AGA}}$  Models

$T$ K	$p$ MPa	$\rho$ kg·m <sup>-3</sup>	$\Delta_{\text{GERG}}$	$\Delta_{\text{AGA}}$
450.000	36.9403	168.101	0.0431	-0.0157
450.000	34.4352	159.226	0.0394	-0.0199
450.000	29.9369	142.164	0.0330	-0.0302
450.001	24.3790	119.036	0.0229	-0.0433
450.001	19.9807	99.206	0.0181	-0.0437
450.001	15.5599	78.108	0.0124	-0.0388
450.001	11.6124	58.543	0.0092	-0.0306
450.001	9.8430	49.631	0.0069	-0.0283
450.001	7.9627	40.110	0.0053	-0.0255
450.000	3.8585	19.316	0.0035	-0.0181
450.001	1.9914	9.925	0.0081	-0.0069
350.000	37.0936	229.895	0.0916	-0.0997
350.000	34.6421	220.377	0.0826	-0.0913
350.000	28.7546	193.928	0.0472	-0.0802
350.000	24.4387	170.726	0.0183	-0.0843
350.000	19.2978	138.398	-0.0091	-0.0997
349.999	15.6452	112.633	-0.0188	-0.0999
349.999	11.9588	85.178	-0.0191	-0.0849
350.000	10.0193	70.561	-0.0167	-0.0732
350.000	6.9664	47.870	-0.0123	-0.0534
350.000	3.9891	26.600	-0.0071	-0.0325
249.996	37.1731	335.901	0.2737	-0.3875
249.994	29.1294	313.364	0.2674	-0.4826
249.994	24.0459	293.781	0.2267	-0.5656
249.994	19.7908	271.255	0.1371	-0.6668
249.994	16.1100	242.925	-0.0417	-0.8291
249.994	12.1021	191.847	-0.3647	-1.1004
249.994	10.0410	152.577	-0.3359	-1.0961
249.998	33.1811	325.625	0.2667	-0.4397
249.995	29.9927	316.146	0.2600	-0.4812
249.995	24.9551	297.695	0.2237	-0.5626
249.995	20.0269	272.680	0.1280	-0.6759
249.995	16.0270	242.082	-0.0683	-0.8549

model, defined as

$$\text{AAD} = \frac{1}{k} \sum_{i=1}^k \left| 100 \frac{(\rho_{i, \text{exp}} - \rho_{i, \text{EOS}})}{\rho_{i, \text{EOS}}} \right| \quad (10)$$

where the summation is over the  $k$  data points for a given mixture at a particular temperature.

At the highest temperature of 450 K, the data are in good agreement with both models (Figure 1). The AADs over the entire pressure range are 0.0176 %, 0.0169 %, 0.0273 %, and 0.0173 % for the GERG-2004 model for mixtures SNG-1 to SNG-4, respectively (Figure 1a). The deviations systematically increase with pressure and are largest (0.111 % at 37 MPa) for mixture SNG-3 (i.e., the mixture having the highest CS content).

**Table 4.** Experimental  $p$ – $\rho$ – $T$  Data for Mixture SNG-3 and Relative Deviations of the Experimental Data  $\rho$  from Densities Calculated with the GERG-2004  $\rho_{\text{GERG}}$  and AGA-8  $\rho_{\text{AGA}}$  Models

$T$	$p$	$\rho$	$\Delta_{\text{GERG}}$	$\Delta_{\text{AGA}}$
K	MPa	$\text{kg}\cdot\text{m}^{-3}$		
250.001	29.5892	316.378	0.4123	−0.5464
249.999	24.1207	295.746	0.3699	−0.6376
250.000	19.6271	271.962	0.2472	−0.7686
250.000	15.8293	242.109	−0.0011	−0.9824
249.999	11.9635	191.509	−0.4256	−1.3126
249.999	10.0532	154.676	−0.4167	−1.3035
274.997	18.2684	214.148	0.0315	−0.5931
274.997	11.9842	141.209	−0.1158	−0.5867
274.998	10.0194	113.199	−0.0503	−0.4473
274.998	7.9251	84.018	0.0163	−0.2767
274.997	5.9773	59.243	0.0365	−0.1686
274.998	3.9836	36.837	0.0268	−0.1018
274.998	1.9663	17.012	0.0130	−0.0488
349.999	36.1258	227.467	0.1808	−0.0950
349.999	30.2445	202.344	0.1340	−0.0772
349.998	24.3433	171.265	0.0722	−0.0792
349.998	19.1909	138.601	0.0256	−0.0936
349.998	15.5710	112.855	0.0059	−0.0918
349.998	11.7499	84.166	0.0034	−0.0691
349.998	9.5206	67.254	0.0069	−0.0516
349.997	7.8536	54.740	0.0051	−0.0431
349.998	7.6913	53.532	0.0044	−0.0428
349.998	5.7563	39.334	0.0022	−0.0334
349.999	3.9093	26.195	−0.0011	−0.0261
349.999	1.9559	12.818	0.0043	−0.0098
449.998	1.9751	9.894	−0.0010	−0.0148
449.998	1.5996	8.004	−0.0004	−0.0125
449.997	1.1929	5.962	−0.0037	−0.0138
449.999	0.9718	4.854	−0.0038	−0.0127
449.998	0.7949	3.968	−0.0055	−0.0134
449.999	0.5838	2.912	−0.0035	−0.0101
449.998	37.6103	171.315	0.1097	0.0057
449.998	28.8108	138.438	0.0789	−0.0127
449.998	23.8254	117.284	0.0599	−0.0238
449.998	19.8610	99.223	0.0483	−0.0242
449.998	15.7472	79.482	0.0369	−0.0198
449.997	11.9774	60.720	0.0268	−0.0150
449.998	9.7378	49.380	0.0243	−0.0100
449.998	6.8363	34.587	0.0147	−0.0120
449.999	3.9014	19.637	0.0082	−0.0117

The deviations approach zero at the lowest pressures, as would be expected since both the experimental system and model approach ideal-gas behavior. (A nonzero intercept would indicate a molar mass for the measured mixture different from that calculated from the assumed composition; this result provides

**Table 5.** Experimental  $p$ – $\rho$ – $T$  Data for Mixture SNG-4 and Relative Deviations of the Experimental Data  $\rho$  from Densities Calculated with the GERG-2004  $\rho_{\text{GERG}}$  and AGA-8  $\rho_{\text{AGA}}$  Models

$T$	$p$	$\rho$	$\Delta_{\text{GERG}}$	$\Delta_{\text{AGA}}$
K	MPa	$\text{kg}\cdot\text{m}^{-3}$		
450.000	36.7490	170.596	0.0550	0.0175
450.000	30.0583	145.646	0.0358	−0.0027
450.000	24.8577	123.806	0.0218	−0.0236
450.001	19.4815	99.058	0.0135	−0.0337
450.000	15.4383	79.214	0.0090	−0.0335
450.000	11.7226	60.321	0.0093	−0.0261
450.001	10.0080	51.472	0.0093	−0.0227
450.000	7.7650	39.841	0.0091	−0.0189
449.999	3.9685	20.194	0.0063	−0.0145
449.998	1.9285	9.752	0.0135	−0.0008
349.998	36.5433	232.693	0.1505	−0.0726
349.999	28.8180	199.755	0.0801	−0.0678
350.000	24.6850	177.702	0.0293	−0.0780
349.999	19.6087	145.531	−0.0235	−0.1050
349.999	15.9340	118.896	−0.0407	−0.1134
349.999	11.7268	86.201	−0.0390	−0.1011
349.999	9.7635	70.738	−0.0311	−0.0881
349.999	9.6197	69.609	−0.0336	−0.0902
349.999	6.7910	47.780	−0.0248	−0.0709
349.999	3.9269	26.697	−0.0204	−0.0510
349.999	2.9935	20.108	−0.0184	−0.0430
350.001	1.1726	7.688	−0.0179	−0.0300
350.002	0.9703	6.344	−0.0193	−0.0298
350.001	0.7812	5.095	−0.0208	−0.0298
350.002	0.5960	3.877	−0.0211	−0.0287
250.000	36.9994	338.880	0.3994	−0.3963
250.000	30.4158	322.534	0.4002	−0.5068
249.999	23.9889	300.956	0.3424	−0.6680
250.000	19.9864	282.287	0.2418	−0.8083
250.000	16.0546	255.841	−0.0088	−1.0458
250.000	14.1626	237.621	−0.2497	−1.2567
250.000	12.0864	209.916	−0.6379	−1.6235
250.000	10.0305	170.313	−0.9230	−1.9746

a consistency check on the composition and validates the estimate of the uncertainty in composition.) The AADs for the AGA-8 model are 0.0157 %, 0.0267 %, 0.0142 %, and 0.0195 % for SNG-1 to SNG-4 (Figure 1b). Here, the systematic deviations are largest at (15 to 20) MPa and trend to smaller values as the pressure is further increased.

The results for the 350 K isotherms are shown in Figure 2a for the GERG-2004 model. The agreement is very good up to pressures of about 20 MPa (AAD of 0.0029 %, 0.0134 %, 0.0068 %, and 0.0173 % for mixtures SNG-1 to SNG-4 for  $p < 20$  MPa), but the data are systematically higher than the model at higher pressures. The AADs taken over all pressures are 0.0058 %, 0.0336 %, 0.0409 %, and 0.0349 %. The largest deviation of +0.182 % is seen for SNG-3 at  $p = 36$  MPa. A comparison of the 350 K data with the AGA-8 model is

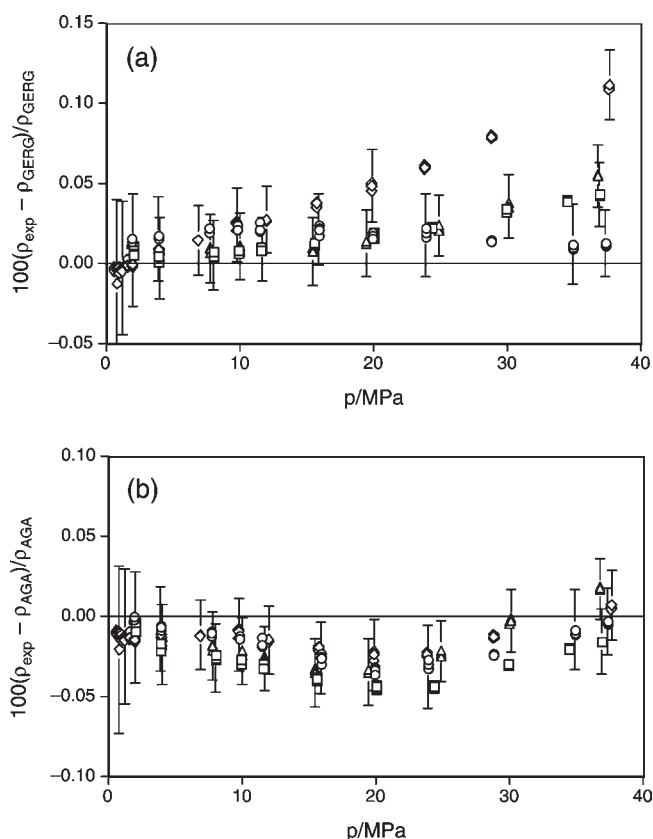


**Figure 1.** Relative deviations of the experimental densities  $\rho_{\text{exp}}$  from the densities calculated with the models  $\rho_{\text{model}}$  at 450 K; (a) GERG-2004 model; (b) AGA-8 model;  $\circ$ , SNG-1;  $\square$ , SNG-2;  $\diamond$ , SNG-3;  $\triangle$ , SNG-4. The error bars depict expanded ( $k = 2$ ) uncertainties; for clarity these are shown for only a subset of data points.

shown in Figure 2b. A systematic deviation with a sigmoidal shape is seen for all four mixtures, with the largest deviations near 16 MPa. The AAD are 0.0157 %, 0.0267 %, 0.0142 %, and 0.0195 %. The largest deviation is  $-0.115$  % for SNG-4 at 16 MPa.

The experimental uncertainties for the SNG-3 isotherm at 350 K at pressures of  $5.7 \text{ MPa} \leq p \leq 24.4 \text{ MPa}$  are substantially larger than for the other pressures (see Figure 2a,b). These were due to a leaking valve. The operation of the densimeter is largely automated; the leak developed overnight and was not corrected until the next day, after data for several pressures were measured. The steady downward drift in pressure and density while the valve was leaking resulted in large values for the standard deviations for the multiple pressures and weighings recorded for a single density determination. The symmetrical weighing design<sup>5</sup> (whereby each sinker and calibration mass was weighed twice in a time-symmetrical pattern for each density determination) largely compensates for this drift, however, and the deviations from the models are seen to be consistent with those for  $p \geq 30 \text{ MPa}$  and  $p \leq 4 \text{ MPa}$ . Replicate density determinations at a given pressure are also seen to have only slightly higher scatter (0.0013 % standard deviation in replicate measurements during the leak compared to 0.0001 % at higher and lower pressures). This result illustrates the value of the symmetrical weighing design and also the value of a thorough uncertainty analysis in revealing possible experimental problems.

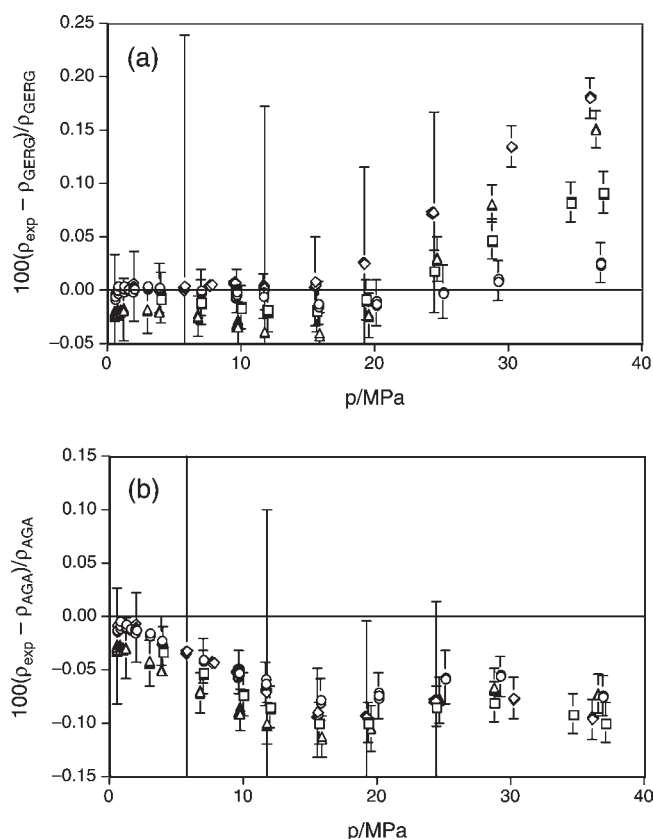


**Figure 2.** Relative deviations of the experimental densities  $\rho_{\text{exp}}$  from the densities calculated with the models  $\rho_{\text{model}}$  at 350 K; (a) GERG-2004 model; (b) AGA-8 model; plot symbols are the same as Figure 1.

Comparisons at 250 K (and also at 275 K for SNG-3) are shown in Figure 3. The deviations from the GERG-2004 model are higher for all pressures (Figure 3a) compared to the 350 K and 450 K data. (Note that the scale on the y-axis has changed.) At pressures greater than 15 MPa, the AADs are 0.101 %, 0.191 %, 0.275 %, and 0.279 %, respectively, for mixtures SNG-1 to SNG-4. The deviations increase as the C5 content increases. For  $4 < p < 15 \text{ MPa}$  the deviations are much larger and show no simple trends. Measurements were attempted at  $p \sim 4 \text{ MPa}$  on SNG-2 and SNG-3, but very erratic weighings were observed, indicating probable condensation onto the sinkers, even though the models predicted a vapor-phase state at these pressures. This indicates that the models do not correctly predict the phase boundary (or that the actual mixture had a higher concentration of pentanes than the assumed composition); this point is discussed further by Atilhan et al.<sup>3</sup>

Densities for one mixture (SNG-1) were measured at very low pressures using the low-range pressure transducer (and with a separate sample loading); these give an AAD of 0.0286 % for  $p < 1.6 \text{ MPa}$ . These pressures were below the two-phase region, and the small deviations validate the models at  $T = 250 \text{ K}$  and low pressures. An additional isotherm at  $T = 275 \text{ K}$  was measured over a limited pressure range for SNG-3 because of the difficulties encountered with the  $T = 250 \text{ K}$  isotherm. This isotherm gives an AAD of 0.0415 %.

The qualitative trends for the AGA-8 model at 250 K and 275 K (Figure 3b) are very similar to the GERG-2004 comparisons at pressures less than about 15 MPa, although the deviations are

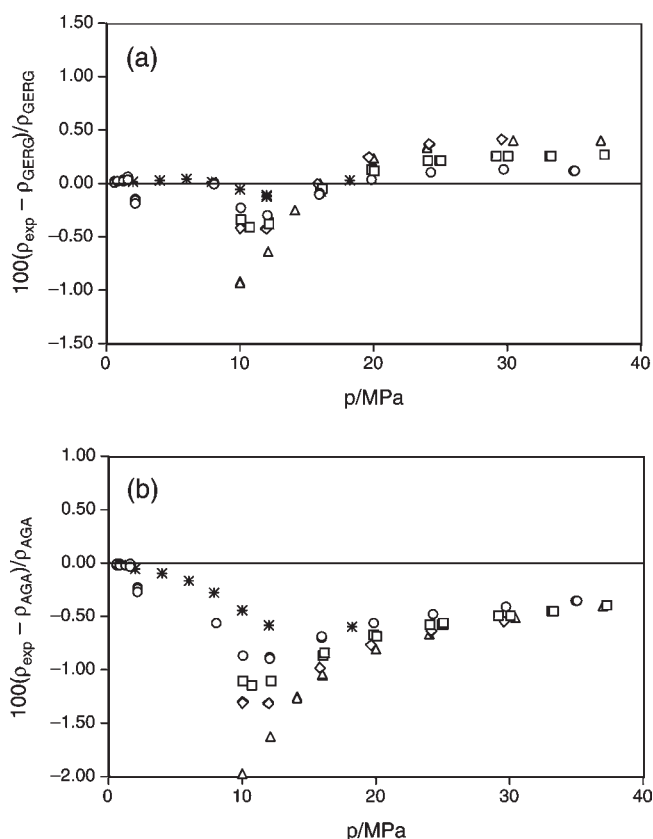


**Figure 3.** Relative deviations of the experimental densities  $\rho_{\text{exp}}$  from the densities calculated with the models  $\rho_{\text{model}}$  at 250 K; (a) GERG-2004 model; (b) AGA-8 model; plot symbols are the same as Figure 1, except for the addition of: \*, SNG-3 at 275 K. The experimental uncertainties are smaller than the plot symbols.

higher. At pressures above 15 MPa, the deviations are systematically negative, in contrast to the positive deviations for the GERG-2004 model. The AADs for  $p > 15$  MPa are 0.491 %, 0.593 %, 0.930 %, and 0.685 % for mixtures SNG-1 to SNG-4. For the  $T = 275$  K isotherm on SNG-3 the AAD was 0.318 %. These deviations are significantly higher than those for the GERG-2004 model.

These comparisons can be summarized as follows. At  $T = 450$  K, both models represent the data within the expanded ( $k = 2$ ) experimental uncertainty, except for the GERG-2004 model at  $p > 20$  MPa for mixture SNG-3 (i.e., the mixture having the highest C5 composition). At  $T = 350$  K, the deviations between experiment and model are within the expanded uncertainty for  $p < 20$  MPa for the GERG-2004 model and  $p < 10$  MPa for the AGA-8 model; the deviations are outside the uncertainty at higher pressures. At  $T = 250$  K, the deviations are substantially larger for both models and are within the experimental uncertainties only at low pressures ( $p < 10$  MPa for the GERG-2004 model and  $p < 3$  MPa for the AGA-8 model). A distinct change in slope in the deviations is seen near  $p = 10$  MPa for both models; this pressure is near the maxcondenbar and indicates a weakness in the models.

## 5. CONCLUSIONS

High accuracy  $p$ – $\rho$ – $T$  data were measured for four synthetic natural-gas-like mixtures. The densities calculated by both the

GERG-2004 and the AGA-8 models are generally very good (average deviations less than 0.05 %) at the higher temperatures ( $T = 350$  K and  $T = 450$  K) and lower pressures ( $p < 15$  MPa). But at higher pressures and lower temperatures, the average deviations are substantially larger, ranging up to 0.28 % and 0.93 % for the GERG 2004 and AGA-8 models, respectively, at  $T = 250$  K and  $p > 15$  MPa for one or more of the mixtures. The higher pressures are of interest for many reservoirs, and temperatures of  $T = 250$  K may be approached in some pipelines. Atilhan et al.<sup>3</sup> present phase-boundary data and  $p$ – $\rho$ – $T$  data at pressures up to 180 MPa on these same mixtures and further discuss the models. This work has examined only four natural-gas-like mixtures, so no definitive conclusions regarding the adequacy of the models can be drawn, but for the four mixtures studied, weaknesses in both models are revealed at temperatures near  $T = 250$  K, especially at pressures near the maxcondenbar.

## ■ ASSOCIATED CONTENT

**S Supporting Information.** The data tabulations in this paper report a single average result at each  $(T, p)$  state point. Three or more replicate measurements were made at each state point, and all of the data are included. More details on uncertainties are provided, including the temperature, pressure, density, composition, and combined uncertainties for each measured point. The standard deviations in the measured quantities (that is, a measure of the scatter in the multiple temperature and pressure readings carried out for each density determination) are also reported. This material is available free of charge via the Internet at <http://pubs.acs.org>.

## ■ AUTHOR INFORMATION

### Corresponding Author

\*E-mail: [markm@boulder.nist.gov](mailto:markm@boulder.nist.gov); tel.: +1-303-497-3580; fax: +1-303-497-5224.

### Author Contributions

Contribution of the National Institute of Standards and Technology.

## ■ REFERENCES

- (1) Kunz, O.; Klimeck, R.; Wagner, W.; Jaeschke, M. *The GERG-2004 Wide-Range Equation of State for Natural Gases and Other Mixtures*, GERG TM15; Fortschritt-Berichte VDI: Weinheim, Germany, 2007; Vol. 6, No. 557.
- (2) Starling, K. E.; Savidge, J. L. *Compressibility factors of natural gas and other related hydrocarbon gases*, Transmission Measurement Committee Report No. 8, Catalog No. XQ9212; American Gas Association: Washington, DC, 1994.
- (3) Atilhan, M.; Aparicio-Martínez, S.; Ejaz, S.; Cristancho, D.; Mantilla, I.; Hall, K. R.  $p\rho T$  behavior of a lean synthetic natural gas mixture using a magnetic suspension densimeter and isochoric apparatus: Part I. *J. Chem. Eng. Data* **2011**, *56*, 212–221.
- (4) Wagner, W.; Kleinrahm, R. Densimeters for very accurate density measurements of fluids over large ranges of temperature, pressure, and density. *Metrologia* **2004**, *41*, S24–S39.
- (5) McLinden, M. O.; Lösch-Will, C. Apparatus for wide-ranging, high-accuracy fluid ( $p$ – $\rho$ – $T$ ) measurements based on a compact two-sinker densimeter. *J. Chem. Thermodyn.* **2007**, *39*, 507–530.
- (6) McLinden, M. O.; Kleinrahm, R.; Wagner, W. Force transmission errors in magnetic suspension densimeters. *Int. J. Thermophys.* **2007**, *28*, 429–448.

(7) McLinden, M. O.; Splett, J. D. A liquid density standard over wide ranges of temperature and pressure based on toluene. *J. Res. Natl. Inst. Stand. Technol.* **2008**, *113*, 29–67.

(8) Moldover, M. R.; McLinden, M. O. Using *Ab Initio* “Data” to Accurately Determine the Fourth Density Virial Coefficient of Helium. *J. Chem. Thermodyn.* **2010**, *42*, 1193–1203.